

Partial Shape Similarity via Alignment of Multi-Metric Hamiltonian Spectra

David Bensaïd

Technion - Israel Institute of Technology

dben-said@campus.technion.ac.il

Amit Bracha

Technion - Israel Institute of Technology

amit.bracha@cs.technion.ac.il

Ron Kimmel

Technion - Israel Institute of Technology

ron@cs.technion.ac.il

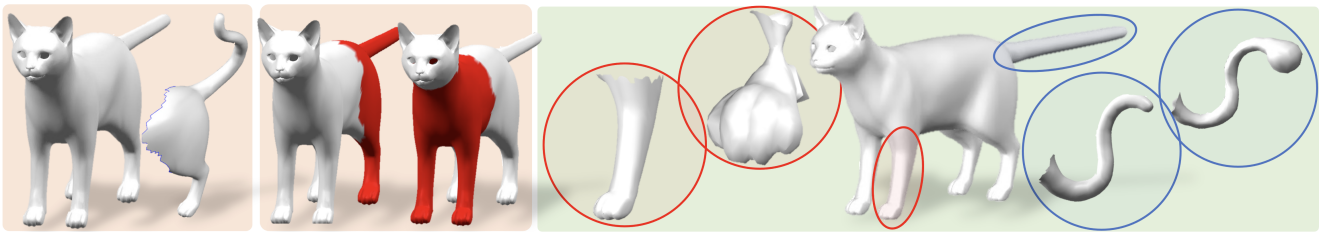


Figure 1: Illustration depicting the benefit of the proposed multi-metric approach for partial shape matching. **Light-Red:** Full and part of a non-rigid shape used for the partial shape matching task (left). The partial shape matching results of the proposed algorithm, which considers a single manifold using both the *scale-invariant* (SI) metric and the *regular* metric, and the [30] algorithm solution to the same problem using only the regular metric (Light-Red-Right). The proposed method successfully matches the partial shape to the full one. **Light-Green:** Canonical embedding of the tail and the foreleg (blue and red ellipses, respectively) under the regular metric and the SI metric (left and right circles, respectively). A leg is similar to the tail when considering the regular metric. The SI metric emphasizes the fine geometric discrepancies between a leg and the tail. These fine details explain the correct matching obtained by the multi-metric approach.

Abstract

Evaluating the similarity of non-rigid shapes with significant partiality is a fundamental task in numerous computer vision applications. Here, we propose a novel axiomatic method to match similar regions across shapes. Matching similar regions is formulated as the alignment of the spectra of operators closely related to the Laplace-Beltrami operator (LBO). The main novelty of the proposed approach is the consideration of differential operators defined on a manifold with multiple metrics. The choice of a metric relates to fundamental shape properties while considering the same manifold under different metrics can thus be viewed as analyzing the underlying manifold from different perspectives. Specifically, we examine the scale-invariant metric and the corresponding scale-invariant Laplace-Beltrami operator (SI-LBO) along with the regular metric and the regular LBO. We demonstrate that the scale-invariant metric emphasizes the locations of important semantic features in articulated shapes. A truncated spectrum of the SI-LBO con-

sequently better captures locally curved regions and complements the global information encapsulated in the truncated spectrum of the regular LBO. We show that matching these dual spectra outperforms competing axiomatic frameworks when tested on standard benchmarks. We introduced a new dataset and compare the proposed method with the state-of-the-art learning based approach in a cross-database configuration. Specifically, we show that, when trained on one data set and tested on another, the proposed axiomatic approach which does not involve training, outperforms the deep learning alternative.

1. Introduction

Non-rigid shape matching is a fundamental task encountered in countless 3D computer vision applications such as augmented reality, medical imaging, and facial recognition. Matching shapes captured in real-world scenarios, where occlusions and partial views inherently occur, is particularly difficult since the former imperfections usually result

in missing geometry. This challenge has motivated a number of recent papers that deal with *partial shape matching* [30, 4, 21, 23, 20, 32].

Matching encompasses two related but distinct notions: *correspondence* and *similarity*. In shape correspondence the matching problem is formulated as a point-wise correspondence between shapes. It is generally solved by aligning local descriptors [17] with a direct [29] or a functional based [32, 21, 20] approach. In contrast, shape similarity adopts a global perspective and maps similar *regions* across a pair of shapes. In a sense, this approach to the matching problem has more to do with the human visual system, which tends to align shapes by association of similar regions rather than points. As a result of its global essence, the similarity formulation is resilient to local discrepancies and is thus well suited for challenging settings such as partiality.

Methods evaluating the similarity of shapes usually rely on *shape descriptors*, which characterize a shape or a part of a shape as a whole. Shape descriptors are generally obtained by aggregating local descriptors [37, 28, 29]. However, their design requires significant tuning efforts, both on local descriptors and on aggregation methods. In 2019, Rampini *et al.* [30] addressed partial shape similarity without local descriptors and suggested the spectrum of the Laplace-Beltrami operator (LBO) as a compact shape descriptor. Similar regions across shapes are then found by formulating and optimizing a spectrum alignment problem. This approach joins a number of recent efforts that consider the spectrum of the LBO for various tasks [12, 25]. In this paper, we address partial shape similarity with a framework that does not require solving dense correspondences and essentially does not rely on local descriptors. The method we introduce generalizes the approach proposed by Rampini *et al.* [30], and considers the spectra of two differential operators defined on a *single* manifold with *multiple* metrics.

The choice of a metric influences fundamental shape properties, including isometry and the notion of similarity itself. Considering the same manifold under different metrics can thus be seen as analyzing the underlying shape from different perspectives. Specifically, we consider the scale-invariant metric and the spectral decomposition of the scale-invariant LBO [3] along with that of the *regular* LBO. Roughly speaking, the LBO spectrum captures the support on which it is defined as a whole. It has therefore a *global* essence that limits its ability to encapsulate fine details [24, 30] that are associated with *local* features. We prove that the spectrum of the scale-invariant LBO is influenced mainly by curved regions which usually contain meaningful details when considering articulated shapes. This property equips the spectrum of the scale-invariant LBO with a particular sensitivity to local curved structures complementing the global shape sensitivity of the spectrum of the regular LBO.

The main contributions of this paper include,

- A novel method for partial shape similarity which exploits the complementary perspectives provided by different choices of a metric for the same manifold.
- A novel interpretation, with a theoretical support, of the scale-invariant metric as a *prior* on the localization of important details in articulated shapes.
- Significant outperforming the competing axiomatic methods and in particular of the single-spectrum framework tested on the standard SHREC'16 Partial Matching Benchmark (CUT).
- The proposed dual spectra method achieves state-of-the-art results in a cross-dataset setup, compared to a state-of-the-art learning based method.

2. Related efforts

Shape matching is a well-established research area and we refer the interested reader to [39] for a comprehensive survey. Recently, learning methods [4] demonstrated remarkable results. Here, we review some recent results related to our line of thought, focusing on *axiomatic* methods for shape matching under partiality.

Spectral methods for partial shape matching. Spectral methods, usually based on the spectral decomposition of the Laplace-Beltrami operator, are ubiquitously used in 3D shape analysis [2]. In 2017, Rodolà *et al.* proposed the first spectral approach for shape matching under partiality, Partial Functional Map (PFM) [32]. PFM extends the seminal framework of functional maps to deal with partiality. Partial shape localization and correspondence are alternatively optimized. Notable follow-up papers include generalizations of PFM to the multipart setting [22, 20] and an iterative refinement procedure [23] that alternates a coarse matching estimated with PFM and an upsampling strategy. Finally, Litany *et al.* [21] proposed a joint diagonalization method to align the spectral basis of a full and a partial shape in the spectral domain. Unlike these methods, we were searching for an approach that would not require solving dense correspondences and would not need local descriptors.

Can you hear the shape of a drum? In 1966, Kac published the seminal paper “Can you hear the shape of a drum?” [19]. There he formulated a central question in geometry processing: Is it possible to recover the exact geometry of a shape from its spectrum?

Two decades later, Gordon *et al.* [15] answered the last question in the negative with a simple pair of non-isometric 2D polygons presenting identical spectra. In 2005, Reuters *et al.* [31] proposed the eigenvalues of the Laplace-Beltrami

operator - called *spectrum* - as a global shape signature. This signature, named ShapeDNA, is simple, compact, and successfully describes important intrinsic properties of natural shapes such as humans and animals. In 2007, the introduction of Global Point Signature (GPS) [33] marked a shift towards spectral signatures, such as the famous Heat Kernel Signature (HKS) [35] and Wave Kernel Signature (WKS) [5], which also involve the *eigenvectors* of the LBO. Unlike ShapeDNA, the latter signatures have theoretical guarantees in a continuous perspective and uniquely define shapes up to isometric transformations. However, local descriptors, like GPS, HKS and WKS, must be associated with aggregation methods, such as the *bag-of-words* [37], to represent an entire shape. They are therefore less suited than the spectrum for more global tasks such as region localization where larger structures, or *regions*, need to be characterized as a whole.

The eigenvalues of the LBO recently regained a great deal of attention in the geometry processing community. While known examples of different manifolds with identical spectra exist, they remain specific and concern 2D polygons [15] and high-dimensional manifolds [9, 18, 10, 38]. At the other end, entire classes of manifolds, such as bi-axially symmetric plane domains [40], have been shown to be fully determined by their spectra. Concerning shapes encountered in real-world scenarios, a line of recent papers based on the spectrum of the LBO demonstrated excellent empirical results. Cosmo *et al.* [12] have shown that the spectrum is informative enough to recover shapes in numerous practical cases, and Moschella *et al.* [25] have learned the joint spectrum of a set of partial shapes without computing the 3D geometry of their union. The basis of our method is the recent approach of Rampini *et al.* [30] who formulated the shape localization problem as a spectrum alignment problem.

Self-functional map. In 2018, Halimi *et al.* [16] proposed the *self-functional map* framework for shape retrieval. It was later extended to shape correspondence [7]. Self-functional maps are compact shape representations that characterize shapes by the inner product of eigenfunctions of Laplace-Beltrami operators induced by two different metrics. The approach of Halimi *et al.* is therefore closely related to our line of thought since it also relies on the analysis of a *single* shape with *multiple* metrics.

3. Background: Laplace-Beltrami and Hamiltonian operators

Shapes as Riemannian manifolds. We model a shape as a Riemannian manifold $\mathcal{M} = (S, g)$, where S is a smooth two-dimensional manifold embedded in \mathbb{R}^3 and g a metric tensor, also referred to as *first fundamental form*. The

metric tensor can be used to define *geometric* quantities on the manifold, such as lengths of curves, and angles between vector fields, and distances between points. Consider a parametric surface $S(u, v) : \Omega \subseteq \mathbb{R}^2 \rightarrow \mathbb{R}^3$, equipped with the regular intrinsic metric g ,

$$(g_{ij}) = \begin{pmatrix} \langle S_u, S_u \rangle & \langle S_u, S_v \rangle \\ \langle S_v, S_u \rangle & \langle S_v, S_v \rangle \end{pmatrix}. \quad (1)$$

An infinitesimal length element ds on the surface S can then be defined by,

$$ds^2 = \mathbf{du}^T(g) \mathbf{du}, \quad (2)$$

with $\mathbf{du} \triangleq \begin{pmatrix} du \\ dv \end{pmatrix}$. Formally, \mathcal{M} is a Riemannian manifold that assigns to every point $m \in \mathcal{M}$ a tangent plane $T_m\mathcal{M}$ and an inner product $\langle \cdot \rangle_g : T_m\mathcal{M} \times T_m\mathcal{M} \rightarrow \mathbb{R}$.

3.1. Laplace-Beltrami operator

The Laplace-Beltrami operator (LBO) Δ_g is an ubiquitous tool in shape analysis that earned the title of ‘‘Swiss army knife’’ in the geometry processing community. The LBO is a generalization of the regular Laplacian operator to Riemannian manifolds. Formally,

$$\Delta_g f \triangleq -\frac{1}{\sqrt{|g|}} \operatorname{div}(\sqrt{|g|} g^{-1} \nabla f), \quad f \in \mathcal{L}^2(\mathcal{M}), \quad (3)$$

where $\mathcal{L}^2(\mathcal{M})$ stands for the Hilbert space of square-integrable scalar functions defined on \mathcal{M} .

Spectral analysis. The semi-positive definite LBO admits the following spectral decomposition with homogeneous Dirichlet boundary conditions,

$$\begin{aligned} \Delta_g \phi_i(x) &= \lambda_i \phi_i(x), & x \in \mathcal{M} \setminus \partial\mathcal{M} \\ \phi_i(x) &= 0, & x \in \partial\mathcal{M} \end{aligned} \quad (4)$$

where $\partial\mathcal{M}$ stands for the boundary of manifold \mathcal{M} . The basis $\{\phi_i\}_{i \geq 0}$ defined by the LBO spectral decomposition is invariant to isometries that may include non-rigid transformations. It is commonly interpreted as a generalization of the Fourier basis on flat domains to Riemannian manifolds [36]. Truncating the basis has been proven to be unique and optimal in approximating smooth functions on a given shape, by which the basis is defined [2].

Discretization. In a discrete setting, S is approximated by a triangulated mesh with n vertices. The discrete LBO can then be approximated by,

$$\mathbf{L} = \mathbf{A}^{-1} \mathbf{W}, \quad (5)$$

where $\mathbf{A} \in \mathbb{R}^{n \times n}$ is known as the *mass matrix* containing an area element about each vertex, while $\mathbf{W} \in \mathbb{R}^{n \times n}$ is the

cotangent weight matrix [27]. The spectral decomposition of the discrete LBO can be computed as a solution for the generalized eigenvalue problem,

$$\begin{aligned} \mathbf{W}\phi_i(x) &= \lambda_i \mathbf{A}\phi_i(x), & x \in \mathcal{M} \setminus \partial\mathcal{M} \\ \phi_i(x) &= 0, & x \in \partial\mathcal{M} \end{aligned} \quad (6)$$

with homogeneous Dirichlet boundary conditions.

3.2. The Hamiltonian operator in shape analysis



Figure 2: Top: First eigenvectors of the LBO of the *partial* shape \mathcal{N} . Bottom: First eigenvectors of the Hamiltonian of the *full* shape \mathcal{M} . The Hamiltonian is defined with a step potential v (in red) corresponding to the effective support of \mathcal{N} . With the adapted potential, the eigenfunctions of the LBO and the Hamiltonian are similar up to their sign.

In 2018, Choukroun *et al.* [11] adapted the well-known Hamiltonian operator from quantum mechanics to shape analysis. The Hamiltonian naturally appears in the celebrated Schrödinger equation that describes the *wave function* of a particle, i.e., its spatial and temporal probability distribution,

$$\begin{aligned} i\hbar \frac{\partial}{\partial t} \Psi(x, y, t) &= \left(\frac{\hbar}{2m} \Delta + V(x, y, t) \right) \Psi(x, y, t) \\ &= H\Psi(t, x, y), \end{aligned} \quad (7)$$

where H is the *Hamiltonian* operator, \hbar the Plank constant, and V a scalar function mapping the domain Ω on which the Schrödinger equation is defined. In the case of a Riemannian manifold, \mathcal{M} , and assuming a time-independent step-potential, the Hamiltonian in Eq. (7) becomes,

$$H_g \triangleq \Delta_g + v, \quad (8)$$

with $v : \mathcal{M} \rightarrow \mathbb{R}$. It is a semi-positive definite operator that admits a spectral decomposition,

$$\begin{aligned} (\Delta_g + v)\phi_i(x) &= \lambda_i \phi_i(x), & x \in \mathcal{M} \setminus \partial\mathcal{M} \\ \phi_i(x) &= 0, & x \in \partial\mathcal{M} \end{aligned} \quad (9)$$

with Dirichlet boundary conditions. Here, λ_i is known as the *energy* of the *wave function* ϕ_i . Using the notations introduced in Section 3, a discrete versions of the Hamiltonian \mathbf{H} and of the related eigendecomposition problem are respectively,

$$\mathbf{H} = \mathbf{A}^{-1}\mathbf{W} + \mathbf{V}, \quad (10)$$

$$\begin{aligned} (\mathbf{W} + \mathbf{A}\mathbf{V})\phi_i(x) &= \lambda_i \mathbf{A}\phi_i(x), & x \in \mathcal{M} \setminus \partial\mathcal{M} \\ \phi_i(x) &= 0, & x \in \partial\mathcal{M}, \end{aligned} \quad (11)$$

where $\mathbf{V} \in \mathbb{R}_+^{n \times n}$ is a diagonal matrix containing the values of the potential v at each vertex of the discretized manifold. We refer the interested reader to [11] for a comprehensive survey of the Hamiltonian operator in the context of shape analysis. For our discussion, the most important property of the Hamiltonian is,

Property 1 *Let \mathcal{M} be a Riemannian manifold and $v : \mathcal{M} \rightarrow \mathbb{R}_+$ a potential function. The eigenfunction ϕ_i of the Hamiltonian exponentially decays in every $\hat{s} \in S$ such that $v(\hat{s}) > \lambda_i$.*

When it comes to shapes, the potential can be considered as a mask determining the domain at which the LBO embedded in the Hamiltonian is effective (see Figure 2). A second key property of the Hamiltonian is the differentiability of its eigenvalues with respect to its potential function [1].

Property 2 *The eigenvalues $\{\lambda_i\}_{i \geq 0}$ of the discretized Hamiltonian operator \mathbf{H} are differentiable with respect to the potential v . Namely,*

$$\frac{\partial \lambda_i}{\partial v} = \mathbf{A}(\phi_i \otimes \phi_i), \quad (12)$$

where \otimes stands for the element-wise multiplication, and ϕ_i is the eigenfunction corresponding to λ_i .

4. Scale-invariant geometry

The search for meaningful representations of images and shapes lays at the heart of computer vision and geometry processing. These representations should be *invariant* to defined classes of transformation such as Euclidean transformations, namely translations, rotations, and scaling. In 2013, Aflalo *et al.* [3] introduced the scale-invariant metric that we summarize next. We refer the reader to the supplementary for a detailed presentation of the scale-invariant metric.

4.1. Scale-invariant metric

The scale-invariant metric for surfaces is based on the Gaussian curvature K [14], which is intuitively related to the *bending* of the surface. The Gaussian curvature depends on

the scale of the shape and the modulation of the Euclidean arc length by \mathbf{K} consequently leads to a *scale-invariant* metric. Using the notations introduced in Section 3, a scale-invariant pseudo-metric \tilde{g} can be defined as,

$$\tilde{g}_{ij} \triangleq |\mathbf{K}| g_{ij}, \quad (13)$$

where g is the *regular* first fundamental form. Remark that the addition of a small positive constant ϵ to the Gaussian curvature in 13 prevents the expression from vanishing and allows the definition of a formal metric. The modulation by the Gaussian curvature shrinks any intrinsically flat region into a point. The LBO of a Riemmanian manifold $\tilde{\mathcal{M}}$ equipped with the scale-invariant metric is called the *scale-invariant Laplace-Beltrami Operator* (SI-LBO) [3]. A closed form of the SI-LBO is derived by plugging the scale-invariant metric \tilde{g} instead of the *regular* metric g into the definition of the LBO,

$$\Delta_{\tilde{g}} f = -\frac{1}{\sqrt{|\tilde{g}|}} \operatorname{div}(\sqrt{|\tilde{g}|} \tilde{g}^{-1} \nabla f), \quad f \in L^2(\tilde{\mathcal{M}}). \quad (14)$$

The discrete version of the SI-LBO and of the related eigen-decomposition problem are respectively,

$$\tilde{\mathbf{L}} = |\mathbf{K}|^{-1} \mathbf{A}^{-1} \mathbf{W}, \quad (15)$$

$$\begin{aligned} (\mathbf{W} + \mathbf{A}|\mathbf{K}|\mathbf{V})\phi_i(x) &= \lambda_i \mathbf{A}|\mathbf{K}|\phi_i(x), & x \in \mathcal{M} \setminus \partial\mathcal{M} \\ \phi_i(x) &= 0, & x \in \partial\mathcal{M}, \end{aligned} \quad (16)$$

where $\mathbf{K} \in \mathbb{R}^{n \times n}$ contains the discrete curvature at the vertices of \mathcal{M} along its diagonal.

4.2. Scale-invariance as a shape prior

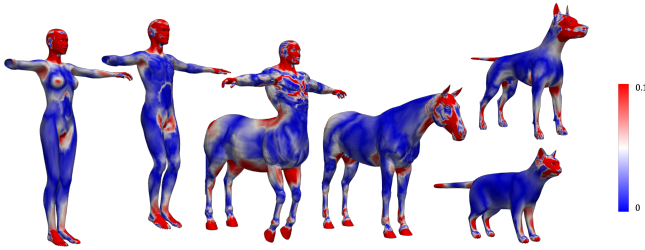


Figure 3: Absolute value of the Gaussian curvature on shapes from TOSCA [8]. The curvature is smoothed for better visualization. Regions with large curvature (in red) have a larger influence on the spectrum of the SI-LBO according to Property 3.

Consider the following interpretation of the scale-invariant metric. The scale-invariant metric can be apprehended as a *prior* on the localization of important semantic

features in articulated shapes such as humans and most animals. Namely, key elements are assumed to be localized in curved regions. Figure 3 shows the curvature on various shapes from SHREC'16 [13]. In the human case for instance, the scale invariant metric *accentuates* the head, the hands and the feet, at the expense of flat regions such as the back and the legs. Intuitively, the scale-invariant metric shrinks intrinsically flat regions into points. Consequently, it focuses on curved regions, see the Supplementary. We formalize this intuition in the spectral domain with a direct generalization of the Weyl law for the SI-LBO.

Lemma 1 *Let $\tilde{\mathcal{M}} = (S : \Omega \subseteq \mathbb{R}^2 \rightarrow \mathbb{R}^3, \tilde{g})$ be a Riemmanian manifold and $\{\tilde{\lambda}_i\}_{i \geq 1}$ the spectrum of the scale-invariant LBO of $\tilde{\mathcal{M}}$. It holds,*

$$\begin{aligned} \tilde{\lambda}_i &\sim \frac{2\pi i}{\int_{\Omega} |\mathbf{K}| da} \\ \text{or, } \tilde{\lambda}_i &\sim \frac{2\pi i}{\operatorname{trace}(|\mathbf{K}|\mathbf{A})} \text{ in the discrete setting.} \end{aligned}$$

Proof (discrete setting). Remark that, in the spectral domain, the introduction of the scale-invariant metric boils down to the substitution of the area matrix \mathbf{A} , that weighs the vertices according to their area, by $|\mathbf{K}|\mathbf{A}$.

The proof in the continuous setting is presented in the Supplementary. A simple perturbation analysis expresses the influence of the curvature on the spectrum of the SI-LBO.

Property 3 *Consider a small perturbation δ_p of the curvature at $p \in \tilde{\mathcal{M}}$. Denote by $\delta K \triangleq \frac{\delta_p}{\operatorname{trace}(|\mathbf{K}|\mathbf{A})}$ the relative perturbation of the curvature and by $\delta \tilde{\lambda} \triangleq \frac{\tilde{\lambda}_i - \tilde{\mu}_i}{\tilde{\lambda}_i}$ the relative perturbation of $\tilde{\lambda}_i$, where $\tilde{\mu}_i$ designates the i^{th} eigenvalue of the perturbed manifold. $\delta \tilde{\lambda}$ respects,*

$$\delta \tilde{\lambda} \sim \delta K.$$

Proof. From Lemma 1,

$$\tilde{\lambda}_i \sim \frac{2\pi i}{\operatorname{trace}(|\mathbf{K}|\mathbf{A})}, \quad \tilde{\mu}_i \sim \frac{2\pi i}{\operatorname{trace}(|\mathbf{K}|\mathbf{A}) + \mathbf{A}_p \delta_p}.$$

$$\begin{aligned} \text{Therefore, } \delta \tilde{\lambda} &\triangleq \frac{\tilde{\lambda}_i - \tilde{\mu}_i}{\tilde{\lambda}_i} \\ &\sim \frac{1}{\tilde{\lambda}_i} \frac{2\pi i \mathbf{A}_p \delta_p \mathbf{A}_p}{\operatorname{trace}(|\mathbf{K}|\mathbf{A})(\operatorname{trace}(|\mathbf{K}|\mathbf{A}) + \mathbf{A}_p \delta_p)} \\ &\sim \frac{1}{\tilde{\lambda}_i} \frac{2\pi i}{\operatorname{trace}(|\mathbf{K}|\mathbf{A})} \frac{\mathbf{A}_p \delta_p}{\operatorname{trace}(|\mathbf{K}|\mathbf{A})} \\ &\sim \mathbf{A}_p \delta \mathbf{K} \end{aligned}$$

Property 3 implies that the spectrum of the SI-LBO is mostly determined by curved regions. Empirically, this property also extends to the modes of the SI-LBO and the basis induced by the spectral decomposition of the SI-LBO is more concentrated, or *compressed*, in curved regions (see Supplementary). Modes related to the first eigenvalues of the SI-LBO capture fine structures, such as fingers. An interesting parallel can thus be drawn between the SI-LBO and differential operators with *compressed modes* [26, 11, 24] tailored to describe local functions on shapes. Unlike those operators, the SI-LBO has the key advantage to be unsupervised and to determine axiomatically the regions where localized spectral analysis should be performed.

5. Method

We propose a framework to find the effective support of a partial shape in a full shape.

Overview. Using Property 1, we reduce the localization of a *partial* shape within a *full* shape to a search for a Hamiltonian’s potential corresponding to the effective support of the partial shape. The search for the potential function is formulated with a cost function promoting the alignment of the spectra of the Hamiltonian defined on the full shape and the LBO defined on the partial shape. Finally, Property 2 allows the minimization of the cost function with a first-order optimization algorithm. Although the problem of aligning spectra is non-convex, Rampini *et al.* [30] have empirically shown that known optimization algorithms can be used to find *good* local minima.

A dual look on a single manifold. We jointly process Riemannian manifolds representing a *single* manifold equipped with *multiple* metrics. Essential shape properties, including the notion of similarity itself, are affected by the choice of a metric and a pair of manifolds can be both isometric and non-isometric according to different metrics [16]. Considering multiple metrics can therefore be viewed as considering alternative perspectives of the same manifold, each being sensitive to distinct types of deformation. Specifically, we use the *regular* and the scale-invariant metrics. As discussed earlier (see Section 4.2), the scale-invariant spectrum incorporates local information from key regions that complement the global perspective of the regular spectrum.

Problem formulation. We formulate the partial shape similarity problem as a region localization task. We consider a full and a partial manifold denoted respectively by S_f and S_p . They define a full and a partial shape up to a metric choice. The output of the proposed framework is an indicator function indicating the *region* of the full shape cor-

responding to the partial shape. Formally, the output scalar function $o : S_f \rightarrow \{1, 0\}$ should respect,

$$S' \sim S_p \quad (17)$$

where $S' = \{x \in S_f \mid o(x) = 1\}$ and \sim stands for an isometry relation according to the *regular* Riemannian metric.

Notations. We denote the full shape equipped with the *regular* metric by $\mathcal{M} = (S_f, g)$ and the spectrum of the Hamiltonian defined over \mathcal{M} by $\{\lambda_i\}_{i=1}^k$ with $\lambda_1 \leq \dots \leq \lambda_k$. $\tilde{\mathcal{M}} = (S_f, \tilde{g})$ stands for the full shape defined with the scale-invariant metric and $\{\tilde{\lambda}_i\}_{i=1}^k$, with $\tilde{\lambda}_1 \leq \dots \leq \tilde{\lambda}_k$, for the spectrum of the *scale-invariant Hamiltonian*. We denote by $\Phi \in \mathbb{R}^{n \times k}$ and $\tilde{\Phi} \in \mathbb{R}^{n \times k}$ the k first eigenfunctions of the Hamiltonian and of the scale-invariant Hamiltonian of \mathcal{M} . In the same way, the partial shape equipped with the *regular* and the scale-invariant metrics are referred to as $\mathcal{N} = (S_p, g)$, $\tilde{\mathcal{N}} = (S_p, \tilde{g})$. The spectra of the LBO and of the SI-LBO are respectively denoted by $\{\mu_i\}_{i=1}^k$ and by $\{\tilde{\mu}_i\}_{i=1}^k$, with $\mu_1 \leq \dots \leq \mu_k$ and $\tilde{\mu}_1 \leq \dots \leq \tilde{\mu}_k$.

Cost function. We consider a cost function promoting the alignment of the spectra of the LBO and of the SI-LBO of \mathcal{N} with the the spectra of the regular and the scale-invariant Hamiltonian of \mathcal{M} . Namely,

$$f(V) = \|\lambda(V) - \mu\|_w^2 + \|\tilde{\lambda}(V) - \tilde{\mu}\|_w^2. \quad (18)$$

Following [30], the weighted L2 norm $\|\cdot\|_w$ is defined as,

$$\|a - b\|_w^2 = \sum_{i=1}^k \frac{1}{b_i^2} (a_i - b_i)^2, \quad (19)$$

to mitigate the weight given to high frequencies.

Optimization. The cost function Eq. (18) induces a constrained optimization problem,

$$\arg \min_{v \geq 0} f(V). \quad (20)$$

According to Property 2, the gradient of the last equation with respect to v is,

$$\nabla_v f = 2(\Phi \otimes \Phi)((\lambda - \mu) \otimes \mu^2) + 2(\tilde{\Phi} \otimes \tilde{\Phi})(\tilde{\lambda} - \tilde{\mu}) \otimes \tilde{\mu}^2. \quad (21)$$

To simplify the optimization process, we minimize an unconstrained relaxation of Eq. (20) instead,

$$\arg \min_V f(q(V)), \quad (22)$$

with $q : \mathbb{R} \rightarrow \mathbb{R}_+$ a smooth function acting element-wisely. We consider $q_1(x) = x^2$ as well as $q_2(x) = c(\tanh(v) + 1)$ with $c \gg \mu_k$. By promoting high step potentials, the saturation function q_2 [30] limits the eigenfunctions that can be considered within the region where $v \approx 0$. Eq. (22) is finally minimized with a trust-region method, a classical first order optimization algorithm.

6. Experiments

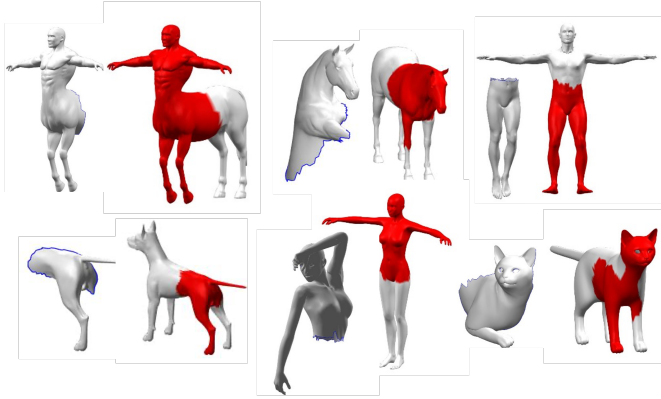


Figure 4: Successful examples of the proposed method on shapes from SHREC'16 [13]. Red regions on the full shapes indicate the regions associated with queried parts.

Method	mean IoU
Bag of words based on SHOT [37]	0.453
PFM [32]	0.563
Rampini <i>et al.</i> [30]	0.676
Proposed dual spectra method	0.757

Table 1: Results of the proposed method, the Bag-of-words baseline [37] and recent axiomatic approaches [30, 32] tested on SHREC'16 (CUTS) [13]. The proposed method outperforms all the competing axiomatic frameworks and achieves state-of-the-art results.

Datasets. We evaluate the proposed method on two databases. The first is the **SHREC'16 Partial Matching Benchmark (CUTS)**, a standard dataset used to assess partial non-rigid shape matching frameworks. The benchmark contains 120 partial shapes from 8 classes (dog, horse, wolf, cat, centaur, and 3 human subjects). The partial shapes are obtained by cutting full shapes that have undergone various non-rigid transformations with random planes. The second is **FAUST-CUTS**, a dataset based on FAUST [6], that we introduce to assess the performance of partial shape matching frameworks in a cross-database configuration. Our in-

tention is to permit a fair comparison between different methods, by introducing new shapes, previously unseen by any learning method, with possibly different discretizations. FAUST-CUTS contains 25 partial shapes from 10 human subjects. We refer the reader to the Supplementary for further details on the dataset and its construction.

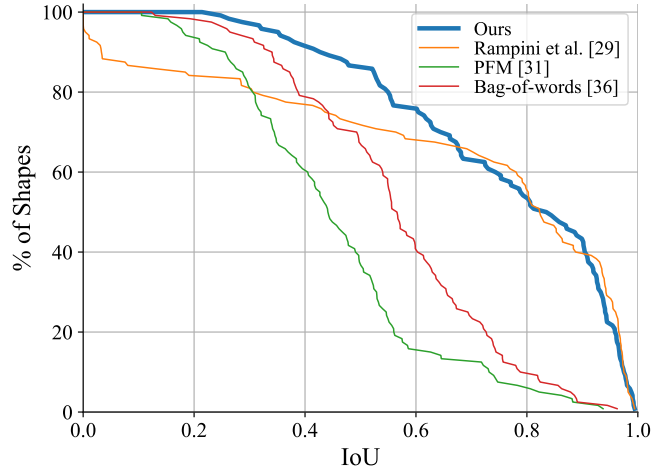


Figure 5: Comparison of the proposed method with recent frameworks [32, 30] and a bag-of-words [37] of SHOT descriptors [34] as a baseline. The graph shows the cumulative score of each method over SHREC'16 (CUTS).

Results. We compare the proposed method with recent axiomatic frameworks for partial similarity on SHREC'16 (CUTS) [13]. We consider the spectrum alignment procedure proposed by Rampini *et al.* [30], Partial Functional Maps (PFM) [32] and a Bag-of-words approach [37] with SHOT descriptors [34]. We use the original code released by the authors and apply the best reported hyperparameters. Table 1 and Figure 5 display a quantitative comparison, showing that the proposed method achieves significantly better results than other axiomatic methods. Figure 4 presents successful examples of the proposed method on shapes from SHREC'16 [13]. Figure 6 analyzes failure cases that mostly arise due to similarity of distinct parts of human and animal bodies such as the torso and back (human) or front and back legs (quadrupeds).

Ablation study. We compare the performance of the proposed framework when considering (1) 20 eigenvalues of the LBO and 20 eigenvalues of the SI-LBO (2) 40 eigenvalues of the LBO (without including the SI-LBO). A comparison of results obtained by (1) and (2) is displayed in Figure 7. Note that for a fair comparison between these methods, an equal total number of eigenvalues is required. The region search is thus performed via alignment problems

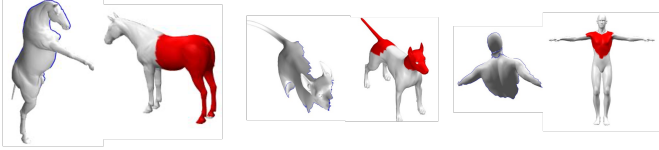


Figure 6: Analysis of failure cases. **Left:** For quadrupeds, the distinction between cuts that contain both back or front legs, versus cuts that contain a back and a front leg, is a challenging task. **Middle:** Partial success on a challenging cut. **Right:** Human back and torso have close LBO and SI-LBO spectra. As a result, the proposed algorithm converges to a wrong local minimum.

that have the same number of constraints. The significantly better performance of (1) highlights the benefits of the proposed multi-metric approach and of the introduction of the scale-invariant metric.

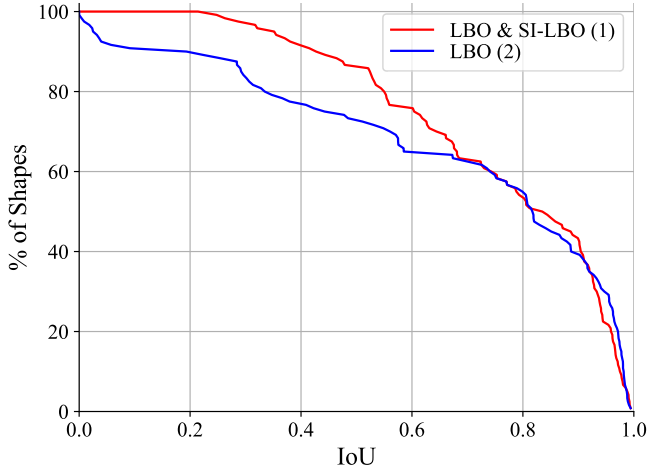


Figure 7: Ablation study. Comparison of the proposed multi-metric framework (1) with a truncated version of the proposed method which only relies on the LBO and its spectrum (2). The graph presents the cumulative scores of (1) and (2) over SHREC'16 (CUTS). (1) reaches a mean IoU of 0.76 and (2) a mean IoU of 0.71.

Cross-dataset generalization & comparison with learning methods. We use FAUST-CUTS to compare the generalization ability of the proposed data-agnostic method with Deep Partial Functional Map (DPFM) [4], the state-of-the-art learning method, trained on SHREC'16. Figure 8 shows that the proposed method significantly outperforms DPFM and displays a clear advantage over actual learning approaches when processing new databases with unfamiliar shapes.

Additional experiments and implementation details of

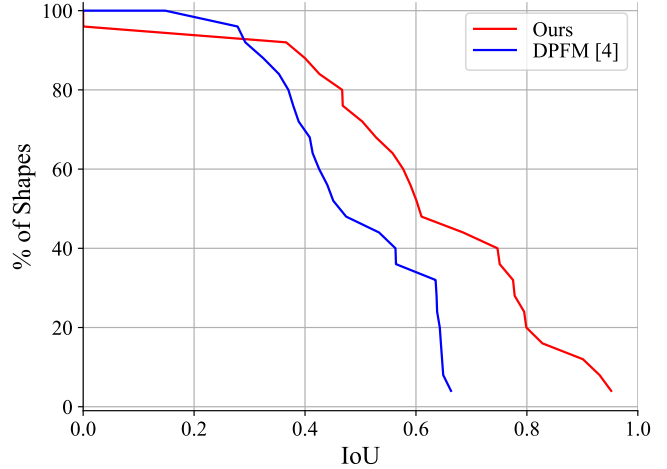


Figure 8: Comparison of the proposed method with Deep Partial Functional Map (DPFM) [4] on the newly introduced FAUST-CUTS dataset. DPFM is the state-of-the-art learning method. It is trained on SHREC'16. The proposed axiomatic approach significantly outperforms DPFM on the FAUST-CUTS dataset. It demonstrates that the proposed method enjoys better generalization properties.

the proposed method can be found in the Supplementary.

7. Future research directions

We introduced a new approach for partial shape similarity. The proposed method exploits the complementary perspective provided by the scale-invariant metric to significantly improve the performance reached by alternative methods. One future research direction is the extension of the proposed method to more challenging datasets such as the SHREC'16 Partial Matching Benchmark (HOLES) [13]. This could notably be done by considering new metric spaces as well as other differentiable shape representations that also adopt a multi-metric approach, such as the self-functional maps [16]. Finally, the proposed method is fully differentiable and can potentially be used as an *unsupervised loss* to improve deep learning setups for partial shape matching.

Acknowledgement. We would like to thank Alon Zvirin for his assistance.

References

- [1] Karim T Abou-Moustafa. 1 differentiating eigenvalues and eigenvectors. 2009. 4
- [2] Yonathan Aflalo, Haim Brezis, and Ron Kimmel. On the optimality of shape and data representation in the

- spectral domain. *SIAM Journal on Imaging Sciences*, 8(2):1141–1160, 2015. 2, 3
- [3] Yonathan Aflalo, Ron Kimmel, and Dan Raviv. Scale invariant geometry for nonrigid shapes. *SIAM Journal on Imaging Sciences*, 6(3):1579–1597, 2013. 2, 4, 5
- [4] Souhaib Attaiki, Gautam Pai, and Maks Ovsjanikov. Dpfm: Deep partial functional maps. In *2021 International Conference on 3D Vision (3DV)*, pages 175–185. IEEE, 2021. 2, 8
- [5] Mathieu Aubry, Ulrich Schlickewei, and Daniel Cremers. The wave kernel signature: A quantum mechanical approach to shape analysis. In *2011 IEEE international conference on computer vision workshops (ICCV workshops)*, pages 1626–1633. IEEE, 2011. 3
- [6] Federica Bogo, Javier Romero, Matthew Loper, and Michael J Black. Faust: Dataset and evaluation for 3d mesh registration. In *Proceedings of the IEEE conference on computer vision and pattern recognition*, pages 3794–3801, 2014. 7
- [7] Amit Bracha, Oshri Halimi, and Ron Kimmel. Shape correspondence by aligning scale-invariant LBO eigenfunctions. 2020. 3
- [8] Alexander M Bronstein, Michael M Bronstein, and Ron Kimmel. *Numerical geometry of non-rigid shapes*. Springer Science & Business Media, 2008. 5
- [9] Robert Brooks. Constructing isospectral manifolds. *The American Mathematical Monthly*, 95(9):823–839, 1988. 3
- [10] Roberts Brooks and Richard Tse. Isospectral surfaces of small genus. *Nagoya Mathematical Journal*, 107:13–24, 1987. 3
- [11] Yoni Choukroun, Alon Shtern, Alex Bronstein, and Ron Kimmel. Hamiltonian operator for spectral shape analysis. *IEEE transactions on visualization and computer graphics*, 26(2):1320–1331, 2018. 4, 6
- [12] Luca Cosmo, Mikhail Panine, Arianna Rampini, Maks Ovsjanikov, Michael M Bronstein, and Emanuele Rodolà. Isospectralization, or how to hear shape, style, and correspondence. In *Proceedings of the IEEE/CVF Conference on Computer Vision and Pattern Recognition*, pages 7529–7538, 2019. 2, 3
- [13] Luca Cosmo, Emanuele Rodola, Michael M Bronstein, Andrea Torsello, Daniel Cremers, and Y Sahillioglu. Shrec’16: Partial matching of deformable shapes. *Proc. 3DOR*, 2(9):12, 2016. 5, 7, 8
- [14] Manfredo P Do Carmo. *Differential geometry of curves and surfaces: revised and updated second edition*. Courier Dover Publications, 2016. 4
- [15] Carolyn S Gordon. You can’t hear the shape of a manifold. In *New Developments in Lie Theory and Their Applications*, pages 129–146. Springer, 1992. 2, 3
- [16] Oshri Halimi and Ron Kimmel. Self functional maps. In *2018 International Conference on 3D Vision (3DV)*, pages 710–718. IEEE, 2018. 3, 6, 8
- [17] Paul Heider, Alain Pierre-Pierre, Ruosi Li, and Cindy Grimm. Local shape descriptors, a survey and evaluation. In *Proceedings of the 4th Eurographics conference on 3D Object Retrieval*, pages 49–56, 2011. 2
- [18] Akira Ikeda. On lens spaces which are isospectral but not isometric. In *Annales scientifiques de l’École Normale Supérieure*, volume 13, pages 303–315, 1980. 3
- [19] Mark Kac. Can one hear the shape of a drum? *The american mathematical monthly*, 73(4P2):1–23, 1966. 2
- [20] Or Litany, Emanuele Rodolà, Alex Bronstein, Michael Bronstein, and Daniel Cremers. Partial single-and multishape dense correspondence using functional maps. In *Handbook of Numerical Analysis*, volume 19, pages 55–90. Elsevier, 2018. 2
- [21] Or Litany, Emanuele Rodolà, Alexander M Bronstein, and Michael M Bronstein. Fully spectral partial shape matching. In *Computer Graphics Forum*, volume 36, pages 247–258. Wiley Online Library, 2017. 2
- [22] Or Litany, Emanuele Rodola, Alexander M Bronstein, Michael M Bronstein, and Daniel Cremers. Non-rigid puzzles. In *Computer Graphics Forum*, volume 35, pages 135–143. Wiley Online Library, 2016. 2
- [23] Simone Melzi, Jing Ren, Emanuele Rodola, Abhishek Sharma, Peter Wonka, and Maks Ovsjanikov. Zoomout: Spectral upsampling for efficient shape correspondence. *arXiv preprint arXiv:1904.07865*, 2019. 2
- [24] Simone Melzi, Emanuele Rodolà, Umberto Castellani, and Michael M Bronstein. Localized manifold harmonics for spectral shape analysis. In *Computer Graphics Forum*, volume 37, pages 20–34. Wiley Online Library, 2018. 2, 6
- [25] Luca Moschella, Simone Melzi, Luca Cosmo, Filippo Maggioli, Or Litany, Maks Ovsjanikov, Leonidas Guibas, and Emanuele Rodolà. Learning spectral unions of partial deformable 3d shapes. 2022. 2, 3

- [26] Vidvuds Ozoliņš, Rongjie Lai, Russel Caflisch, and Stanley Osher. Compressed modes for variational problems in mathematics and physics. *Proceedings of the National Academy of Sciences*, 110(46):18368–18373, 2013. [6](#)
- [27] Ulrich Pinkall and Konrad Polthier. Computing discrete minimal surfaces and their conjugates. *Experimental mathematics*, 2(1):15–36, 1993. [4](#)
- [28] Jonathan Pokrass, Alexander M Bronstein, and Michael M Bronstein. A correspondence-less approach to matching of deformable shapes. In *International Conference on Scale Space and Variational Methods in Computer Vision*, pages 592–603. Springer, 2011. [2](#)
- [29] Jonathan Pokrass, Alexander M Bronstein, and Michael M Bronstein. Partial shape matching without point-wise correspondence. *Numerical Mathematics: Theory, Methods and Applications*, 6(1):223–244, 2013. [2](#)
- [30] Arianna Rampini, Irene Tallini, Maks Ovsjanikov, Alex M Bronstein, and Emanuele Rodola. Correspondence-free region localization for partial shape similarity via hamiltonian spectrum alignment. In *2019 International Conference on 3D Vision (3DV)*, pages 37–46. IEEE, 2019. [1](#), [2](#), [3](#), [6](#), [7](#)
- [31] Martin Reuter, Franz-Erich Wolter, and Niklas Peinecke. Laplace–beltrami spectra as ‘shape-dna’ of surfaces and solids. *Computer-Aided Design*, 38(4):342–366, 2006. [2](#)
- [32] Emanuele Rodolà, Luca Cosmo, Michael M Bronstein, Andrea Torsello, and Daniel Cremers. Partial functional correspondence. In *Computer graphics forum*, volume 36, pages 222–236. Wiley Online Library, 2017. [2](#), [7](#)
- [33] Raif M Rustamov et al. Laplace-beltrami eigenfunctions for deformation invariant shape representation. In *Symposium on geometry processing*, volume 257, pages 225–233, 2007. [3](#)
- [34] Samuele Salti, Federico Tombari, and Luigi Di Stefano. Shot: Unique signatures of histograms for surface and texture description. *Computer Vision and Image Understanding*, 125:251–264, 2014. [7](#)
- [35] Jian Sun, Maks Ovsjanikov, and Leonidas Guibas. A concise and provably informative multi-scale signature based on heat diffusion. In *Computer graphics forum*, volume 28, pages 1383–1392. Wiley Online Library, 2009. [3](#)
- [36] Gabriel Taubin. A signal processing approach to fair surface design. In *Proceedings of the 22nd annual conference on Computer graphics and interactive techniques*, pages 351–358, 1995. [3](#)
- [37] Roberto Toldo, Umberto Castellani, and Andrea Fusiello. A bag of words approach for 3d object categorization. In *International Conference on Computer Vision/Computer Graphics Collaboration Techniques and Applications*, pages 116–127. Springer, 2009. [2](#), [3](#), [7](#)
- [38] Hajime Urakawa. Bounded domains which are isospectral but not congruent. In *Annales scientifiques de l’École Normale Supérieure*, volume 15, pages 441–456, 1982. [3](#)
- [39] Oliver Van Kaick, Hao Zhang, Ghassan Hamarneh, and Daniel Cohen-Or. A survey on shape correspondence. In *Computer graphics forum*, volume 30, pages 1681–1707. Wiley Online Library, 2011. [2](#)
- [40] Steve Zelditch. Spectral determination of analytic bi-axisymmetric plane domains. *Geometric & Functional Analysis GAFA*, 10(3):628–677, 2000. [3](#)